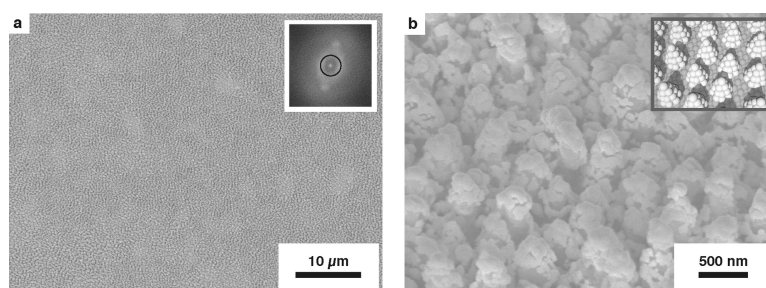


## Femtosecond Laser-Nanostructured Substrates for Surface-Enhanced Raman Scattering

Eric D. Diebold, Nathan H. Mack, Stephen K. Doorn, and Eric Mazur

*Langmuir*, 2009, 25 (3), 1790-1794 • DOI: 10.1021/la803357q • Publication Date (Web): 09 January 2009

Downloaded from <http://pubs.acs.org> on February 24, 2009



### More About This Article

Additional resources and features associated with this article are available within the HTML version:

- Supporting Information
- Access to high resolution figures
- Links to articles and content related to this article
- Copyright permission to reproduce figures and/or text from this article

# Femtosecond Laser-Nanostructured Substrates for Surface-Enhanced Raman Scattering

Eric D. Diebold,<sup>†</sup> Nathan H. Mack,<sup>‡</sup> Stephen K. Doorn,<sup>‡</sup> and Eric Mazur<sup>\*†</sup>

School of Engineering and Applied Sciences, Harvard University, Cambridge, Massachusetts 02138, and Chemistry Division, Los Alamos National Laboratory, Los Alamos, New Mexico 87545

Received October 10, 2008

We present a new type of surface-enhanced Raman scattering (SERS) substrate that exhibits extremely large and uniform cross-section enhancements over a macroscopic (greater than 25 mm<sup>2</sup>) area. The substrates are fabricated using a femtosecond laser nanostructuring process, followed by thermal deposition of silver. SERS signals from adsorbed molecules show a spatially uniform enhancement factor of approximately 10<sup>7</sup>. Spectroscopic characterization of these substrates suggests their potential for use in few or single-molecule Raman spectroscopy.

## Introduction

Since its discovery in 1977,<sup>1,2</sup> surface-enhanced Raman scattering (SERS) has provided a glimpse into the future of high-throughput single-molecule detection and analysis. The wealth of vibrational spectroscopic information offered by Raman spectroscopy makes it ideal for highly multiplexed bioassays and label-free analyte detection schemes that are not possible using the current state-of-the-art molecular dye and quantum-dot-based fluorescence techniques. Ordinarily, the cross section for a molecular Raman transition is extremely small, but nanostructured SERS substrates can enhance Raman signals to a level that is competitive with well-established fluorescence techniques. For example, using nanoparticle-based SERS substrates, single-molecule detection has been reported.<sup>3,4</sup> Despite this achievement, the current dearth of reliable and reproducible substrates with both large-scale uniformity and large enhancement factors has severely limited the use of SERS in most applications.

Metallic nanoparticles, patterned on solid substrates or aggregated from colloidal solutions, exhibit large SERS enhancement factors.<sup>5–7</sup> While nanoparticle-based systems are often difficult to control in terms of signal homogeneity and particle stability, and are not typically appropriate for use in large area assays, they offer insight into the requirements for a suitable SERS substrate. The giant signal enhancements observed in these nanoparticle systems are typically dominated by the large electric fields generated in so-called “hot spots” that exist in the regions between two (or more) adjacent particles.<sup>8</sup> By optimizing the number, density, and field intensity enhancement of these hot spots, SERS substrates can provide large, easily

detectable signals for trace detection and identification using Raman spectroscopy.

To overcome the physical limitations inherent to nanoparticle-based SERS systems, attempts have been made to use highly roughened substrates of bulk solid-state materials. For example, metallized porous silicon exhibits SERS properties after proper chemical etching treatment.<sup>9</sup> However, the practicality of these substrates is limited by the mechanical stability<sup>10</sup> of highly porous silicon, making them difficult to integrate into higher-order structures, such as microfluidics-based analytical devices.

Here, we report a technique for fabrication of large area, planar silicon-based SERS substrates that overcomes these physical obstacles. Using a femtosecond laser to nanostructure a silicon surface, we produce SERS substrates that exhibit reproducible and spatially uniform enhancement factors of approximately 2 × 10<sup>7</sup> at an excitation wavelength of 632.8 nm. This enhancement decreases slowly with increasing excitation wavelengths, maintaining significant enhancement (about 10<sup>6</sup>) out to 900 nm. In addition to the large enhancement factor, these substrates can easily be patterned in a variety of form factors over large areas.

## Experiment

**SERS Substrate Fabrication.** All substrates were fabricated using a femtosecond laser structuring process on an n-type silicon (100) wafer ( $\rho = 0.005 - 0.020 \Omega \cdot \text{cm}$ ). A pulse train from a regeneratively amplified titanium:sapphire laser was used to generate 800-nm center wavelength, 100-fs pulses at a repetition rate of 1 kHz. This pulse train was frequency-doubled to a center wavelength of 400 nm using a thin BiBO<sub>3</sub> crystal. The second harmonic pulse width exiting the crystal was less than 200 fs. These laser pulses were loosely focused with a plano-convex lens to achieve an average fluence of 10 kJ/m<sup>2</sup> at the surface of a silicon wafer fastened to the inside of a 10-mm deep cuvette filled with deionized water. The cuvette was mounted on a computer-controlled two-axis translation stage and rastered at an appropriate speed such that each point on the silicon wafer was subjected to approximately 500 pulses.

To render the surfaces SERS-active, silver was thermally evaporated onto the structured silicon. Using a quartz crystal microbalance to measure the thickness of a planar continuous film, substrates were fabricated with 10, 30, 60, 80, 100, and 200 nm of deposited silver. All films were thermally evaporated at a rate of 0.15 nm/s, with no heating or cooling applied to the substrate during deposition.

(9) Chan, S.; Kwon, S.; Koo, T. W.; Lee, L. P.; Berlin, A. A. *Adv. Mater.* **2003**, *15*, 1595.

(10) Sharma, S. N.; Sharma, R. K.; Bhagavannarayana, G.; Samanta, S. B.; Sood, K. N.; Lakshmikummar, S. T. *Mater. Lett.* **2006**, *60*, 1166.

\* To whom correspondence should be addressed. E-mail: mazur@seas.harvard.edu.

<sup>†</sup> Harvard University.

<sup>‡</sup> Los Alamos National Laboratory.

(1) Jeanmaire, D. L.; Van Duyne, R. P. *J. Electroanal. Chem.* **1977**, *84*, 1.

(2) Albrecht, M. G.; Creighton, J. A. *J. Am. Chem. Soc.* **1977**, *99*, 5215.

(3) Kneipp, K.; Wang, Y.; Kneipp, H.; Perelman, L. T.; Itzkan, I.; Dasari, R.; Feld, M. S. *Phys. Rev. Lett.* **1997**, *78*, 1667.

(4) Nie, S. M.; Emery, S. R. *Science* **1997**, *275*, 1102.

(5) Van Duyne, R. P.; Hulstee, J. C.; Treichel, D. A. *J. Chem. Phys.* **1993**, *99*, 2101.

(6) Freeman, R. G.; Grabar, K. C.; Allison, K. J.; Bright, R. M.; Davis, J. A.; Guthrie, A. P.; Hommer, M. B.; Jackson, M. A.; Smith, P. C.; Walter, D. G.; Natan, M. J. *Science* **1995**, *267*, 1629.

(7) Kneipp, K.; Kneipp, H.; Itzkan, I.; Dasari, R. R.; Feld, M. S. *Chem. Rev.* **1999**, *99*, 2957.

(8) Campion, A.; Kambampati, P. *Chem. Soc. Rev.* **1998**, *27*, 241.

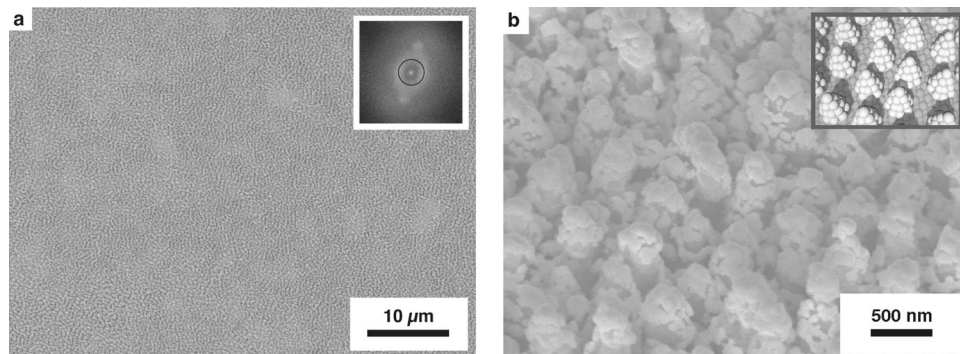


**Figure 1.** Scanning electron microscope images of the nanostructured substrate coated with 80 nm of silver. (a) Normal and (b) side ( $45^\circ$ ) views of the surface. Insets: (a) FFT of the normal image. The black ring indicates the peak position in the FFT intensity, which corresponds to a spatial period of 505 nm. (b) Schematic diagram of the geometrical model used for surface area enhancement calculation.

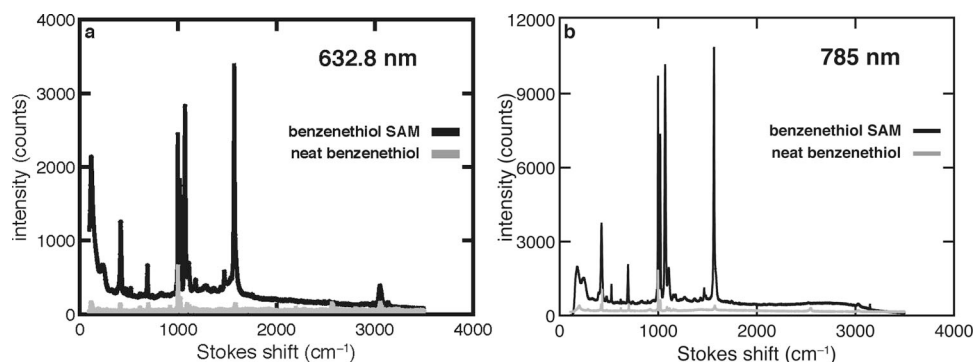


**Figure 2.** Raman spectra of benzenethiol taken with (a) 5 mW 632.8 nm excitation, and (b) 10 mW 785 nm excitation. The SERS spectra (black) in both panels a and b were taken from a SAM adsorbed on a substrate with an 80 nm silver film applied. The corresponding unenhanced Raman spectra (gray) of neat benzenethiol are shown for comparison. All spectra were recorded with an integration time of 1 s.

The pristine silver surfaces were then functionalized with a self-assembled monolayer (SAM) of benzenethiol or mercaptobenzoic acid. The silver-coated substrates were submerged in 4-mM solutions made with ethanol for 1 h and then gently rinsed in neat ethanol for 1 min, followed by drying under a stream of nitrogen. These analytes were chosen as they are nonresonant with the Raman excitation sources used in this work, and readily form uniform SAMs on clean silver surfaces.

**Raman Spectroscopy.** Multiple Raman setups were used to characterize the SERS properties of these substrates. Enhancement factor estimates as well as point-to-point variations in intensity over the patterned area were measured on a micro-Raman apparatus. Using a 5-mW, s-polarized 632.8-nm HeNe laser, spectra were recorded through a  $10\times$  microscope objective (0.25 NA) and projected onto a thermoelectrically cooled charge-coupled device (CCD) array using a 1200-g/mm diffraction grating. Individual spectra were recorded from both single spots ( $1.6\text{-}\mu\text{m}$  diameter) on the substrate, and from a  $500\text{-}\mu\text{m}$  thick cell of neat benzenethiol for normalization. The same apparatus was used to measure the SERS uniformity over a  $500\text{-}\mu\text{m} \times 600\text{-}\mu\text{m}$  area from points on the substrate spaced  $5\text{-}\mu\text{m}$  apart using a 0.5-s integration time per spectrum. Raman spectra were also collected using a second micro-Raman apparatus, which employed a 10-mW s-polarized 785-nm laser diode, a  $20\times$  microscope objective (0.40 NA), a 1200-g/mm diffraction grating, and a thermoelectrically cooled CCD array.

Raman excitation profiling was accomplished using a tunable continuous-wave titanium:sapphire laser in a backscattering configuration. The incident beam was focused onto the sample through an  $f = 0.1$  m lens to yield a spot size of approximately  $20\text{-}\mu\text{m}$ . The incident laser wavelengths were varied from 700 to 900 nm in 5-nm increments with the power held constant at 15 mW, as measured at the sample. The SERS signal was collected through a triple monochromator and then recorded on a back illuminated, deep depletion CCD array. The excitation profile intensities for the  $1075\text{-}\text{cm}^{-1}$  mercaptobenzoic acid band were corrected for instrument

response using the nearby  $1105\text{-}\text{cm}^{-1}$  band from the normal (unenhanced) Raman spectrum of 4-acetamidophenol taken under identical conditions.

**Electron Microscopy.** Secondary electron microscope images of the substrates were collected using a field-emission gun scanning electron microscope, utilizing an accelerating voltage of 5 kV. No additional sample preparation was performed prior to imaging the substrates.

## Results

Figure 1a shows a typical scanning electron micrograph of the laser-fabricated surface after silver deposition. The structuring procedure results in a quasi-uniform distribution of raised features on the silicon surface. A fast Fourier transform (FFT) of the image (Figure 1a, inset) exhibits a ring with a peak intensity corresponding to a surface feature periodicity of 505 nm. Although the cones protrude above the surface of the silicon by as much as  $1\text{-}\mu\text{m}$ , the underlying silicon wafer is left intact and structurally unchanged.<sup>11</sup> After deposition of a silver thin film, the surface of the substrate is covered with highly nonuniform silver nanoparticles, whose dimensions are typically on the order of 50–100 nm (Figure 1b). These silver particles provide an appropriate surface on which to form a SAM of either benzenethiol or mercaptobenzoic acid.

We obtained the SERS spectra shown in Figure 2 from a benzenethiol SAM on a substrate coated with 80 nm of silver at two different excitation wavelengths (632.8 and 785 nm). Spectra recorded under identical conditions from a region of the silicon wafer that was not laser structured (i.e., a flat silver

(11) Shen, M. Y.; Crouch, C. H.; Carey, J. E.; Mazur, E. *Appl. Phys. Lett.* **2004**, *85*, 5694.

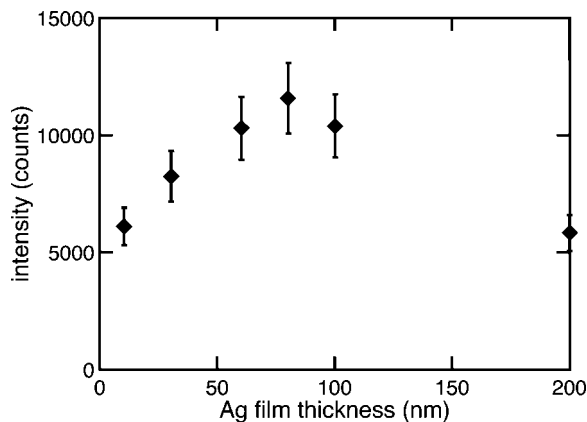


**Figure 3.** Dependence of the integrated intensity of the  $1572 \pm 10 \text{ cm}^{-1}$  band of benzenethiol on the deposited silver film thickness. The values shown are the average of the integrated Raman intensity collected with 5 mW 632.8 nm excitation for 1 s from 10 randomly chosen locations on each  $2 \text{ mm} \times 2 \text{ mm}$  sample.

substrate) result in no observable signal (data not shown). The SERS signal shows no discernible dependence on the sample orientation with respect to the excitation laser polarization. In both panels a and b of Figure 2, the absence of Raman bands at  $917 \text{ cm}^{-1}$  and  $2567 \text{ cm}^{-1}$  (S–H in-plane bending and S–H stretching modes, respectively) indicates that a single monolayer of benzenethiol is adsorbed on the surface.<sup>12</sup> For comparison, unenhanced Raman spectra, obtained from a neat solution of benzenethiol in a glass cell, are also shown in Figure 2a,b. On the basis of these data, the average SERS cross-section enhancement factor for the  $1572 \text{ cm}^{-1}$  normal mode is approximately  $2 \times 10^7$  and  $1 \times 10^6$  for 632.8 and 785 nm excitation, respectively.

The SERS intensity depends on the amount of silver deposited on the structured silicon surface. Figure 3 shows the integrated intensity of the  $1572 \pm 10 \text{ cm}^{-1}$  (C–C stretch) Raman band from a SAM of benzenethiol applied to different substrates with varying silver thicknesses. Each data point shown is the average of 10 randomly sampled locations on each substrate. Under otherwise identical conditions, with 632.8 nm excitation and a  $10\times$  (0.25 NA) microscope objective, the SERS intensity is greatest for substrates with 80 nm of silver. The enhancement factor of the sample with an 80 nm film is roughly a factor of 2 greater than that of the samples with 10 and 200 nm thick films.

We measured the uniformity of the SERS intensity over a large area of the substrate coated with 80 nm of silver using 632.8 nm excitation. We created a Raman map (Figure 4a) using the integrated intensity of the  $1572 \pm 10 \text{ cm}^{-1}$  Raman band of benzenethiol. The greatest deviation from the point of maximum signal is  $-4.3 \text{ dB}$ , with a standard deviation of 0.125 (map intensity normalized to its mean). This uniformity is reproducible from substrate to substrate, as demonstrated by the SERS signal intensities from 42 different samples. Using the same experimental setup, a single Raman spectrum was taken from a randomly chosen location on each  $2 \text{ mm} \times 2 \text{ mm}$  sample. The integrated intensity of the  $1572 \pm 10 \text{ cm}^{-1}$  band in these 42 spectra has a standard deviation of 0.129 (distribution normalized to its mean). Histograms of the intensities of both the SERS map and the 42 individual samples are shown in Figure 4b. An F-test of the standard deviations of the two distributions indicates that their difference is not statistically significant ( $p = 0.88$ ).

The SERS enhancement observed from these substrates is remarkably constant with respect to excitation wavelength. Figure

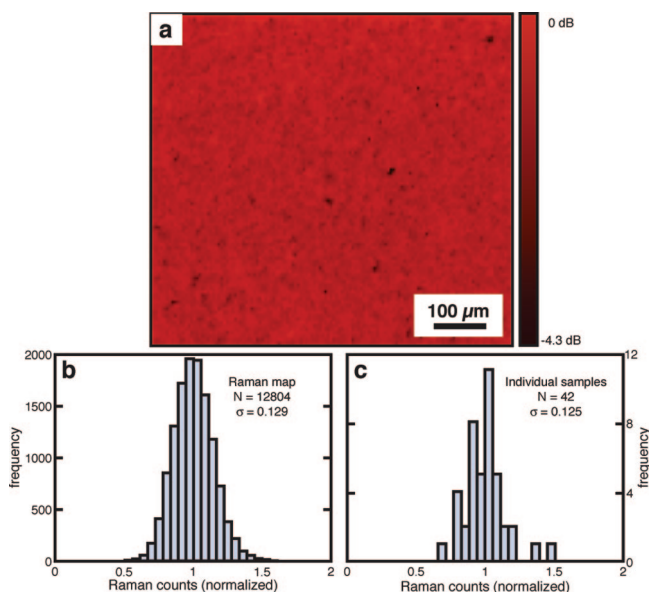


**Figure 4.** (a) Raman map of a  $500 \mu\text{m} \times 600 \mu\text{m}$  area of a substrate with an 80 nm silver film. The map is obtained from the integrated intensity of the  $1572 \pm 10 \text{ cm}^{-1}$  band of a benzenethiol SAM adsorbed on the substrate. Each point in the map was taken using 5 mW 632.8 nm excitation with a 0.5 s integration time. (b) Histogram of the intensity from the map shown in panel a. (c) Histogram of the SERS intensities recorded from randomly chosen locations on 42 different  $2 \text{ mm} \times 2 \text{ mm}$  samples using 1 s integration times.

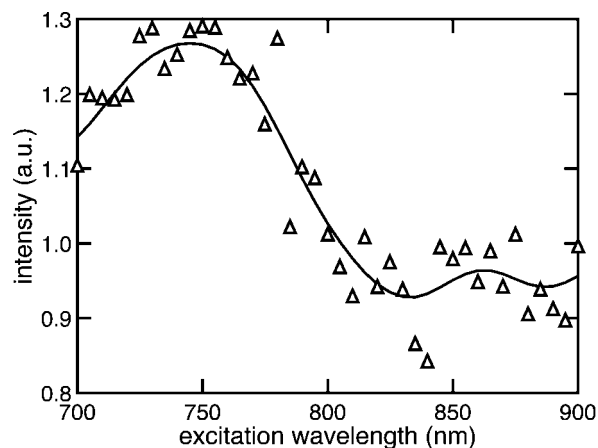


**Figure 5.** Relative integrated intensity of the  $1075 \pm 10 \text{ cm}^{-1}$  band of a mercaptobenzoic acid SAM deposited on a sample with an 80-nm silver coating, as a function of excitation wavelength. Spectra taken at each wavelength were collected with 15 mW excitation for an integration time of 2 min. The curve shown is an FFT smoothing of the data.

5 shows the integrated intensity of the  $1075 \text{ cm}^{-1}$  band of mercaptobenzoic acid over a range of excitation wavelengths using a substrate with an 80 nm silver film. An FFT filter removed high-frequency noise and smoothed the data. Within the experimental excitation wavelength range (700–900 nm), the maximum SERS enhancement occurs near 750 nm. However, the maximum is not exceptionally pronounced, as the signal at 750 nm is only 30% greater than the signal at 850 nm.

## Discussion

Over the past decade, silicon surfaces have been structured using femtosecond laser pulses under many different experimental

conditions.<sup>13</sup> The resulting surface morphology is governed by several factors, including the laser wavelength, pulse duration, fluence, and the structuring environment. For example, cones formed in an aqueous environment are approximately an order of magnitude smaller in height and width than cones formed in a gaseous environment.<sup>14,15</sup> X-ray photoelectron spectroscopy reveals that the cones produced in this work are covered by a thin layer of SiO<sub>2</sub>.<sup>11</sup> This layer has roughness on the order of tens of nanometers<sup>11,14</sup> and enables a unique thin film deposition process that is responsible for the SERS properties observed in these samples. The rough surface acts as a physical catalyst for silver particle formation by enabling a reduction of the silver/SiO<sub>2</sub> interfacial surface energy during the deposition process.<sup>16</sup> Instead of the smooth continuous film that results during metal film deposition on flat surfaces, we observe discontinuous, particulate film deposition on the nanostructured silicon substrates. As shown in Figure 1b, the deposited silver does not form a continuous film, but rather a collection of aggregated particles—an architecture which is generally accepted to greatly enhance Raman signals from molecules nearby or adsorbed to the surface.<sup>17–20</sup>

The Raman scattering cross-section enhancement factor (EF) for the substrate is determined from  $EF = (I_{SERS}/I_{Neat})(N_{Neat}/N_{SERS})$ , where  $I_{SERS}$  and  $I_{Neat}$  are the integrated intensities of a specific Raman band, normalized to the incident laser photon flux for the cases of the SERS substrate with the SAM applied and the neat molecular dye, respectively. Proper enhancement factor calculations must also account for the number of probed molecules,  $N_{SERS}$  and  $N_{Neat}$ , in each sample. For  $N_{SERS}$ , the benzenethiol SAM density ( $6.8 \times 10^{14} \text{ cm}^{-2}$ ) and the laser spot size give an estimate of the maximum number of molecules on a planar surface that can contribute to the SERS signal.<sup>21</sup> However, the surface of the substrates is not planar, and the effective benzenethiol SAM density must be adjusted by a surface area enhancement factor, which takes into account the morphology of the substrates. The simplest model of the surface is to assume an array of silicon cones with an average period of 505 nm, as shown in Figure 1a. The surface is modeled as a quasi-ordered array of cones<sup>13</sup> covered with a layer of spherical silver particles, whose total cross-sectional area is equivalent to the surface area of the cones (Figure 1b, inset). This geometrical model results in a surface area enhancement of approximately 10. The number of probed molecules in the unenhanced sample of neat benzenethiol,  $N_{Neat}$ , is approximated using the molecular weight and density of benzenethiol and the effective interaction volume of the Gaussian laser beam with the neat benzenethiol sample. The confocal nature of the micro-Raman spectrometer is incorporated in the determination of  $N_{Neat}$  by accounting for the axial collection efficiency of the microscope, which was rigorously measured using standard procedures.<sup>22,23</sup>

When calculating the enhancement factor for these substrates, we assumed that all molecules on the surface Raman scatter with equal efficiency. However, nanoparticle SERS studies have shown that the relatively few molecules residing in the hot spots between particles contribute predominantly to the SERS signal.<sup>24,25</sup> This observation suggests that these nanostructured substrates exhibit small regions of enormous Raman enhancement, with the average surface enhancement factor being on the order of  $10^7$  (the focused 632.8 nm laser beam waist of approximately  $1.6 \mu\text{m}$  is large enough to generate intense Raman scattering from many hot spots at once, considering the surface features' size and spacing). This enhancement factor is believed to be sufficient to observe single-molecule SERS using modern Raman spectrometers.<sup>22</sup>

Thin film deposition of silver on SiO<sub>2</sub> substrates presents numerous opportunities from which to control the morphology of the resulting films, and by extension, the resulting SERS activity. Deposition parameters such as substrate temperature, deposition rate, and vacuum pressure can be used to alter a variety of thin film properties (i.e., thickness, grain size, and surface roughness). Keeping other parameters constant, we optimized the signal from these nanostructured substrates by varying the amount (thickness) of deposited silver. Silver is known to follow Volmer–Weber growth processes on oxide surfaces resulting in small silver clusters that grow into islands on the surface.<sup>26</sup> The deposited film thickness determines the density and size of the silver particles formed on the surface. It should be noted that no special deposition requirements are necessary to generate particles with SERS relevant dimensions (50–100 nm) on the nanostructured substrates, even at film thicknesses that would normally cross far above the percolation threshold to form a continuous silver film on a planar SiO<sub>2</sub> substrate.<sup>27</sup> As shown in Figure 3, an 80 nm film of silver creates an optimal distribution of particles on the surface for 632.8 nm excitation. Plasmon resonances of these particle aggregates result in large local field enhancements and thus large SERS signals from adsorbed molecules. The dependence on silver thickness can be explained based on the particulate nature of the silver films: too little deposited silver results in a surface sparsely covered with isolated particles, and a corresponding decrease in SERS signal. Additionally, too much deposited silver forms a near-continuous film on the surface, covering the nanoscale features of the silicon substrate, leading to a decreased SERS signal.

In addition to the large enhancement factors observed using these substrates, the SERS signal measured over a large area of a single substrate (Figure 4b), as well as the signal measured from substrate to substrate (Figure 4c) is extremely uniform. Statistical analysis of these data indicates that large substrates can be reproducibly fabricated in mass quantities. The uniformity of these substrates is largely a function of the laser fabrication process used to produce the nanostructured surface. During fabrication, the focused femtosecond laser beam (full width at half-maximum (fwhm) =  $80 \mu\text{m}$ ) used to structure the silicon is rastered across the surface with enough overlap between subsequent passes ( $40 \mu\text{m}$ ) to create a uniformly patterned substrate with no unexposed silicon surfaces. The typical spot sizes of the continuous wave lasers (632.8 and 785 nm) used to measure SERS signals from these substrates are significantly smaller ( $<5 \mu\text{m}$ ) than the structuring laser spot size. The uniform

(13) Tull, B. R.; James, E.; Carey, E. M.; McDonald, J.; Yalisove, S. M. *Mater. Res. Soc. Bull.* **2006**, *31*, 626.

(14) Crouch, C. H.; Carey, J. E.; Warrender, J. M.; Aziz, M. J.; Mazur, E.; Genin, F. Y. *Appl. Phys. Lett.* **2004**, *84*, 1850.

(15) Sheehy, M. A.; Winston, L.; Carey, J. E.; Friend, C. A.; Mazur, E. *Chem. Mater.* **2005**, *17*, 3582.

(16) Smith, D. L., *Thin-Film Deposition: Principles and Practice*; McGraw-Hill: New York, 1995.

(17) Michaels, A. M.; Jiang, J.; Brus, L. *J. Phys. Chem. B* **2000**, *104*, 11965.

(18) Munro, C. H.; Smith, W. E.; Garner, M.; Clarkson, J.; White, P. C. *Langmuir* **1995**, *11*, 3712.

(19) Kerker, M.; Siiman, O.; Wang, D. S. *J. Phys. Chem.* **1984**, *88*, 3168.

(20) Bergman, J. G.; Chemla, D. S.; Liao, P. F.; Glass, A. M.; Pinczuk, A.; Hart, R. M.; Olson, D. H. *Opt. Lett.* **1981**, *6*, 33.

(21) McFarland, A. D.; Young, M. A.; Dieringer, J. A.; Van Duyne, R. P. *J. Phys. Chem. B* **2005**, *109*, 11279.

(22) Ru, E. C. L.; Blackie, E.; Meyer, M.; Etchegoin, P. G. *J. Phys. Chem. C* **2007**, *111*, 13794.

(23) Cai, W. B.; Ren, B.; Li, X. Q.; She, C. X.; Liu, F. M.; Cai, X. W.; Tian, Z. Q. *Surf. Sci.* **1998**, *406*, 9.

(24) Kneipp, K.; Wang, Y.; Kneipp, H.; Itzkan, I.; Dasari, R. R.; Feld, M. S. *Phys. Rev. Lett.* **1996**, *76*, 2444.

(25) Fang, Y.; Seong, N. H.; Dlott, D. D. *Science* **2008**, *321*, 388.

(26) Venables, J. A.; Spiller, G. D. T.; Hanbucken, M. *Rep. Prog. Phys.* **1984**, *47*, 399.

(27) Yoshida, S.; Yamaguchi, T.; Kinbara, A. *J. Opt. Soc. Am.* **1971**, *61*, 62.

SERS intensities observed in this work using high spatial resolution Raman microscopes implies that the SERS enhancement is free from any spatial periodicity due to the finite size of the structuring laser's beam. We expect the SERS enhancement of these substrates to maintain this level of uniformity over any macroscopic distance, assuming the structuring laser output and silver deposition conditions are consistent across the entire structured area. In principle, these substrates are limited only by the size of the silicon wafer, the travel of the translation stages used during fabrication, and the size of the evaporator used to deposit the silver film.

The broad range of excitation wavelengths over which these nanostructured substrates provide significant enhancement affords great flexibility for use with a wide range of laser excitation sources for SERS or surface-enhanced resonance Raman spectroscopy (SERRS). The position and width of the peak in the excitation profile shown in Figure 5 indicates there is an optimal excitation wavelength within the probed range. However, the relatively featureless nature of the excitation profile implies that the substrates may be suitable for operation over a much broader range of excitation wavelengths than probed in this measurement. The enhancement factor at 632.8 nm is more than an order of magnitude greater than the enhancement factor at 785 nm. This difference illustrates that the maximum in the excitation profile is merely a local maximum within the probed wavelength range. This maximum in the near-infrared portion of the spectrum is consistent with the typical spectral position of a surface plasmon resonance of aggregated silver nanoparticles.<sup>21,28,29</sup> In general, aggregation of silver nanoparticles not only red shifts their surface plasmon resonance, but also broadens this resonance over much of the visible range.<sup>30</sup> This broadening may be responsible for the SERS enhancement observed over wide excitation energies in these substrates. This broadband operation allows high-frequency (greater than 3000  $\text{cm}^{-1}$ ) Raman bands to be easily observed in SERS spectra without the typical decrease in intensity seen in many SERS substrates<sup>8</sup> (e.g., Figure 2a. In Figure 2b, taken with 785-nm excitation, the intensity of the Raman bands at frequencies greater than 3000  $\text{cm}^{-1}$  are limited by the efficiency of the silicon-based CCD detector).

The substrates are stable over long periods of time. We formed mercaptobenzoic acid monolayers on pristine substrates 3 months after initial substrate fabrication, and found no noticeable loss

in SERS signal relative to mercaptobenzoic acid monolayers formed on freshly fabricated substrates. Once formed, the monolayers are extremely stable, as their SERS signals remain constant over a period of several months. The stability of the Raman signal is most likely a function of both the unique mechanical stability innate to these nanostructured substrates as well as the molecular composition of the SAM itself. We chose benzenethiol and mercaptobenzoic acid as SERS reporter molecules, as they are known to effectively bind to a silver substrate via thiol moieties.<sup>31</sup> The robust nature of these substrates makes them well suited for integration with highly sensitive spectroscopic devices over long periods of service with little degradation in performance.

## Conclusion

In summary, we present a simple two-step process for fabricating silicon-based SERS substrates. These substrates exhibit extremely large and uniform Raman scattering cross-section enhancement factors over macroscopic areas. The enhancement factor of the substrates depends on the deposited silver film thickness; this parameter determines the spacing and density of silver particles formed on the nanostructured silicon surface. The substrates have an excitation wavelength dependence that is quite flat over the near-infrared range, making them compatible with numerous laser excitation sources. The excellent spatial uniformity, large SERS enhancement, structural stability, and simple fabrication make these substrates attractive candidates for use in large-area trace detection schemes using Raman spectroscopy.

**Acknowledgment.** This work was supported by the Army Research Office, under Contract Nos. N00014-03-M-0325 and W911NF-05-1-0341. E.D.D. fabricated the substrates, and performed Raman spectroscopic measurements. N.H.M. performed the excitation profiling and Raman spectroscopic measurements. S.K.D. and E.M. supervised the research. The authors would like to thank Horiba Jobin Yvon and X. Sunney Xie for use of their laboratories' facilities, and Jessica Watkins for assistance with statistical analysis of the data. All authors contributed to the manuscript. E.D.D. acknowledges support from an NDSEG fellowship. N.H.M. acknowledges support from the LANL Agnew Postdoctoral Fellowship. S.K.D. acknowledges support from the LANL LDRD program.

LA803357Q

(28) Felidj, N.; Aubard, J.; Levi, G.; Krenn, J. R.; Hohenau, A.; Schider, G.; Leitner, A.; Aussenegg, F. R. *Appl. Phys. Lett.* **2003**, *82*, 3095.

(29) Kneipp, K.; Kneipp, H.; Itzkan, I.; Dasari, R. R.; Feld, M. S. *J. Phys.: Condens. Matter* **2002**, *14*, R597.

(30) Kreibig, U.; Genzel, L. *Surf. Sci.* **1985**, *156*, 678.

(31) Bain, C. D.; Troughton, E. B.; Tao, Y. T.; Evall, J.; Whitesides, G. M.; Nuzzo, R. G. *J. Am. Chem. Soc.* **1989**, *111*, 321.